# Input and Design Optimization Under Uncertainty to Minimize the Impact Velocity of an Electrostatically-Actuated MEMS Switch

M. S. Allen* [1], J. E. Massad†, R. V. Field, Jr.† and C. W. Dyck‡

*Engineering Physics Department

University of Wisconsin-Madison

Madison, WI 53706

†Applied Mechanics Development

‡RF / Optoelectronics

Sandia National Laboratories

Albuquerque, NM 87185 [2]

---

**Abstract**

*The dynamic response of a radio-frequency micro-electro mechanical system (RF MEMS) to a time-varying electrostatic force is optimized to enhance robustness to variations in material properties and geometry. The device functions as an electrical switch, where an applied voltage is used to close a circuit. The objective is to minimize the severity of the mechanical impact that occurs each time the switch closes, because severe impacts have been found to significantly decrease the life of these switches. Previous works have demonstrated that a classical vibro-impact model, a single degree-of-freedom oscillator subject to mechanical impact with a single rigid barrier, captures the relevant physics adequately. Certain model parameters are de-*

*scribed as random variables to represent the significant unit-to-unit variability observed during fabrication and testing of a collection of nominally-identical switches; these models for unit-to-unit variability are calibrated to available experimental data. Our objective is to design the shape and duration of the voltage waveform so that impact kinetic energy at switch closure is minimized for the collection of nominally-identical switches, subject to design constraints. A voltage waveform designed using a deterministic model for the RF switch is found to perform poorly on the ensemble. An alternative waveform is generated using the proposed optimization procedure with a probabilistic model, and found to decrease the maximum impact velocity by a factor of two relative to the waveform designed deterministically. The methodology is also applied to evaluate a design change that reduces the impact velocity further and to predict the effect of fabrication process improvements.*

*Key words:* MEMS dynamics, input shaping, nonlinear dynamics, vibro-impact system, reduced-order modeling

---

## 1 Introduction

Radio Frequency Micro Electro-Mechanical System (RF MEMS) switches have been the subject of study for a number of applications because they can potentially provide very low power consumption, high isolation and greater linearity in a compact package [1,2]. Unfortunately, current designs for RF switches fail to achieve the high reliability demanded for many applications. During op-

[1] Corresponding author. Tel.: 608-890-1619, E-mail: msallen@engr.wisc.edu.

[2] Sandia is a multiprogram laboratory operated by Sandia Corporation, a Lockheed Martin Company, for the United States Department of Energy's National Nuclear Security Administration under Contract DE-AC04-94AL85000.

eration, an input voltage is typically applied to close an RF MEMS switch, and the dynamics of the closure event have a significant impact on the performance and design lifetime of a switch. This work seeks to model and optimize the dynamics of an RF MEMS switch while accounting for the considerable unit-to-unit variability inherent in the switches.

The kinetic energy of a switch scales with its velocity, and when a switch closes this energy must be dissipated before the switch obtains a stable, closed state. This was observed experimentally using Laser-Doppler Vibrometry [3]; a switch was shown to bounce on its contacts a number of times before closing. The voltage signal used to close the switch was then replaced with a sequence of pulses that was shown to greatly reduce the velocity with which the switch impacted its electrical contacts and the subsequent bouncing. A high velocity before impact also can lead to higher deformations and hence higher stresses in the device during the close event. These observations motivate the use of shaped voltage waveforms to limit the contact velocities of electrostatically-actuated MEMS devices.

It has proved difficult to design an actuating waveform that is effective for an ensemble of RF MEMS switches manufactured using current processes because there is considerable unit-to-unit variability in the dimensions and the properties of these switches. This work demonstrates that a waveform designed to minimize the contact velocity, or provide a soft landing, for the nominal switch gives poor results when applied to an ensemble of switches with varying parameters. One must consider random variability in order to minimize the contact velocity experienced by the ensemble. This can be cast as a problem of Optimization Under Uncertainty (OUU) or Reliability-Based Design Optimization (RBDO) [4]. This work presents a procedure that can

be used to optimize the actuating waveform to minimize the contact velocity experienced by an ensemble of switches. The procedure is also used to explore alternate designs that reduce the contact velocity further and to study the effect of reducing the unit-to-unit variation due to the manufacturing process.

One very important obstacle to Reliability-Based Design Optimization (RBDO) for the switch of interest is the computational cost required. Most approaches to RBDO require a large number of evaluations of the switch model just to evaluate its uncertainty. This must then be repeated at each iteration of the optimization algorithm. The models initially available for the RF MEMS switch were three-dimensional, finite element models comprising many solid elements totaling hundreds of thousands of degrees of freedom. These models were discussed and compared to experiments in [5]. The computation time for these finite element models is large enough to encumber numerous executions for iterative algorithms. Tests on the physical switches are also very expensive, especially when testing them to failure, so only point validations of the analysis models are possible. The models then must adequately predict the change in the behavior of the switches resulting from changes in a few key geometrical and material properties.

A number of Reliability-Based Design Optimization (RBDO) methods have been presented in recent years, most of which are aimed at reducing the computational cost required to evaluate the function (which may be a finite element code) that relates the uncertain parameters in a system (here considered the inputs) to measures of the system's performance (the outputs). Optimization under uncertainty methodologies can be classified as Robust Design Optimization (RDO) methods or as RBDO methods [4]. The former seek to maximize deterministic performance while minimizing the sensitivity of the optimum

solution to the uncertain parameters. This is done by including the sensitivities in the objective function. The RDO procedure is justified for stochastic systems by noting that the variances of the outputs can be determined from the sensitivities of the inputs if the output function is modeled using a first order Taylor series. Hence minimizing the magnitude of the sensitivities to the inputs tends to minimize the variances of the outputs. RBDO methods incorporate some form of stochastic analysis to optimize statistical measures of performance. The stochastic analysis is usually made tractable by assuming an underlying form, such as a first order Taylor series, for the function that is being optimized. The First- and Second- Order Reliability Methods (FORM and SORM) expand upon this concept by first using a nonlinear optimization routine to find the failure boundary and then compute a Taylor expansion about that point [6]. One potential drawback to this approach is that the iterative search for the most probable point of failure becomes more difficult as the number of uncertain parameters, and hence the dimension of this iterative optimization problem, increases. Also, as with most nonlinear optimization problems, one is rarely guaranteed that global convergence is obtained. Furthermore, one cannot estimate confidence bounds on the results obtained by FORM or other RBDO methods, even if global convergence is obtained. The computational efficiency of this class of RBDO methods diminishes if multiple failure modes are of interest, as is the case in this work, since each typically requires a separate analysis.

Both classes of methods have been successfully applied to MEMS systems, even if none has enjoyed broad application. For example, Han and Kwak [7] used RDO to optimize the design of a MEMS accelerometer and a resonant-type micro probe by simultaneously minimizing their objective function and its

gradient with respect to the random parameters. Wittwer *et al.* [8] computed the first order sensitivities of the force-displacement curve of a bistable MEMS mechanism to various uncertain parameters and used the computed sensitivities in an RBDO approach to estimate the variance of the force-displacement curve. Allen *et al.* [9], used the FORM algorithm to optimize the design of a variable capacitance MEMS capacitor. They first validated the FORM algorithm for their application by comparing it to Monte Carlo Simulation (MCS) and then used it to optimize the design of the capacitor. Allen *et al.* observed that the FORM algorithm worked well even though their system was nonlinear, yet all of the uncertain variables in their system were assumed to be Gaussian with relatively small coefficients of variation. Maute and Frangopol also used the FORM algorithm as part of an optimization strategy for a MEMS device [4].

Another class of RBDO methods are based on statistical sampling, the most common being the Monte Carlo Simulation (MCS) method. The MCS method is widely applicable and very robust. It is valid irrespective of the form of the underlying input-output relationship. Furthermore, one can compute confidence bounds on the statistics estimated using MCS, and the relationship between computational cost and the expected accuracy is clear. Both of these features are highly attractive for this work, since the uncertainty modeling procedure cannot be verified either experimentally or analytically. Furthermore, the objective function encountered in this work is expected to be highly nonlinear due to mechanical impact and the electrostatic force and the uncertainties in the system are large and highly non-Gaussian.

The primary disadvantage of the MCS method is that it may require a large number of evaluations of the objective function, especially if one is concerned

with the tails of a distribution. As a result, the MCS method is not very practical unless one has a computationally efficient system model. This work addresses this by first deriving a simple, computationally efficient model for the physics of interest from the finite element models using a Ritz-type model reduction. The effects of key geometrical parameters on the modes of the Ritz model are captured over the relevant ranges using polynomial series. The limitations and assumptions made during the model reduction process are easy to understand and quantify by interrogating the bandwidth of the forces applied to the system. For example, previous works [3] found that other aspects of the switch's performance improved when the input was shaped [10,11] to limit excitation to higher frequency modes. This would also tend to make the single mode approximation employed here more accurate.

This paper is organized as follows. We first derive a reduced order model that provides a good representation of the dynamics of the RF Switch to an actuating voltage. The objective function and optimization procedure are then discussed and some results presented. Finally, the effects of design and process improvement are illustrated followed by some conclusions.

## 2 RF Switch Model

The RF MEMS switch design of interest is shown in Fig. 1. The switch consists of a stiff gold plate supported above a rigid substrate by four folded leaf springs. A 100 nm thick electrostatic pad is adhered to the substrate below the switch plate to provide electrostatic actuation. When voltage is applied to the pad, the plate deflects downward and the contact tabs make mechanical contact with the transmission lines to close the circuit. Dyck *et al.* describe

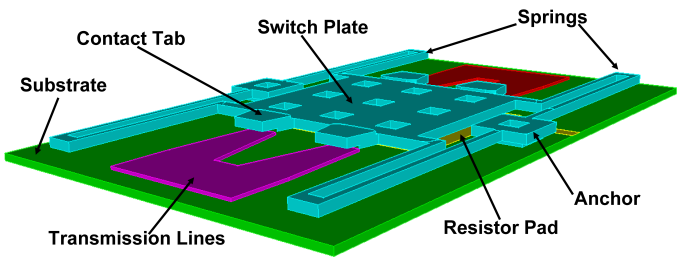


Fig. 1. *Schematic of RF MEMS switch.*

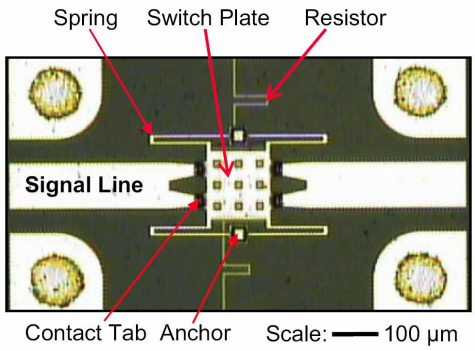


Fig. 2. *Optical Microscope Image of RF MEMS switch.*

the design and characterization of this switch in [12].

### *2.1 Model Reduction*

Experimental measurements on representative switches reveal that the small amplitude response of the switch is dominated by two modes below 300 kHz [13]. These modes occur at roughly 20 and 70 kHz, the first of which is similar to the static deflection shape of the switch in its closed position and the second primarily involves bending of the leaf springs and relatively little displacement of the plate. Previous testing also revealed that the contribution of the second mode could be nearly eliminated by shaping the waveform as shown in Fig. 5. (A more formal input shaping approach such as those in [10] or [11] has not been necessary.) Contact forces applied to the switch plate by the waveguide contacts may also serve to excite the higher modes of the plate, yet these will

be minimal if the velocity of the plate is small enough at impact (*i.e.*, if the voltage waveform optimization is successful.) These observations suggest that the switch can be adequately modeled using a one term Ritz series [14]. The transient response of an actual switch to voltage waveforms was compared to the response of both a single-degree of freedom model and a three-dimensional finite element model in [5]. There, it was observed that the first mode motion of the switch clearly dominates the response. This and other works [3,13,15] have demonstrated the accuracy and the limitations of the reduced order model for individual switches, so a detailed validation of the single-degree of freedom model will not be repeated here. This work is concerned with modeling an ensemble of nominally identical switches, whose parameters are random due to manufacturing variation.

Let $X(t)$ denote the displacement of the contact tabs; the equations of motion are

$$M\,\ddot{X}(t) + K\,X(t) = \frac{\epsilon\,a}{2}\left[\frac{u(t)}{G - X(t)}\right]^2,\ X(0) = \dot{X}(0) = 0, \tag{1}$$

where $M$ and $K$ denote the effective mass and stiffness of the switch plate, respectively. Our convention is to denote all deterministic quantities with lower-case letters or symbols and all random quantities with upper-case letters or symbols. The right hand side of Eq. (1) defines the applied electrostatic force, where $\epsilon$ and $a$ denote the electric permittivity of air and the surface area of the switch plate, respectively, $G$ is the random gap distance between the switch plate and electrostatic pad at $X = 0$, and $u(t)$ is the voltage waveform applied to the pad. Mechanical impact between the contact tabs and waveguide is included by introducing the following kinematic constraint

$$\dot{X}(t^+) = \begin{cases} \dot{X}(t^-) & \text{if } X(t^-) < D, \\ -\eta\, \dot{X}(t^-) & \text{if } X(t^-) = D, \end{cases} \tag{2}$$

where $D$ denotes the random travel distance for switch closure, and $\eta \in (0, 1]$ is the (deterministic) coefficient of restitution. A similar model has been used to study the dynamic response of a collection of MEMS inertial switches [16].

### *2.2 Model Calibration*

The distributions of random variables in Eqs. (1) and (2) must be specified before the model can be used to predict the response of an ensemble of RF switches. This was done by fitting distributions to experimental observations of a small collection of nominally identical switches. Many of the parameters in Eqs. (1) and (2) cannot be measured directly, so some effort was required to obtain them from the measured data. The following experimentally observable quantities have a significant effect on the dynamics of the switch, and have been found to exhibit significant variability: elastic modulus of the switch plate ($E$), electrostatic gap ($G$), plate thickness ($T$) and travel distance ($D$). Measurements of these quantities are shown in Fig. 3 (a)-(d). (The modulus is actually not directly measurable, yet it can be deduced from the pull in voltage $U_{pi}$ as will be explained.) The model calibration procedure consists of first estimating probabilistic models of $E$, $G$, $T$, and $D$ and then relating these quantities to the parameters of Eqs. (1) and (2).

Expert opinion and past experience with the manufacturing process suggest that the distributions of random variables $G$ and $D$ tend to be skewed to

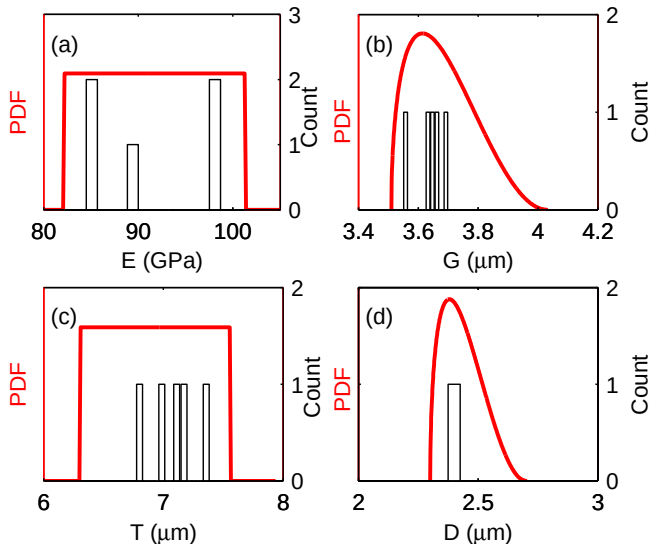


Fig. 3. *Probability Density Functions of and histograms of available data for: (a) elastic modulus of plate, (b) electrostatic gap, (c) plate thickness, and (d) travel distance.*

the right. A Beta distribution was fit to the available data for $G$ and $D$ because its parameters can be chosen so that it describes a slightly skewed yet bounded distribution. Limited information was available for $E$ and $T$, so these were taken to be uniformly distributed in the interval bounded by $\pm 25\%$ of their nominal values. Past experience with the manufacturing process and its predecessors suggests that these uncertainties are reasonable and conservative.

These random variables must now be related to the model parameters in Eqs. (1) and (2). The quasi-static voltage at which the switch closes, dubbed the "pull-in voltage" $U_{pi}$ can be related to the model parameters as follows. The system in Eq. (1) exhibits a snapping phenomenon, in which the linearized stiffness of the switch becomes negative for sufficiently large voltage $u$. The snap through point, found by solving for the position of the switch at which the linearized stiffness changes sign is $X = G/3$. Substituting this position for $X$ in Eq. (1) and neglecting inertia since the pull in tests are performed

quasi-statically, one obtains the following expression for $U_{pi}$

$$U_{pi} = \sqrt{\frac{8}{27}\frac{K\,G^3}{\epsilon\,a}}. \tag{3}$$

The three dimensional static finite element (FEA) model discussed in [5] was used to find the effective stiffness of the switch for various values of the switch thicknesses. The following polynomial relationship between the effective stiffness of the switch and its thickness and modulus was then fit to the FEA results for thickness ranging from 5$\mu$m to 9$\mu$m

$$K\left(E,T\right) = a_2\,E\,T\left(T - a_1\right), \tag{4}$$

where $a_1 = 3.1458$ and $a_2 = 0.027186$ are the coefficients of the polynomial fit. Equation (4) can be substituted into (3) to solve for the modulus in terms of $U_{pi}$, $T$, and $G$. The four parameters defining the switch, $D$, $G$, $T$ and $E$ are assumed to be independent, while it is noted that the procedure for determining $E$ could lead to artificial correlation between them if the measurements or static Finite Element model contain significant errors.

The thickness and modulus of the switches both determine the effective stiffness of the single degree of freedom model through Eq. (4). The effective mass is found using the following procedure. A dynamic finite element model was used to determine the following relationship between the natural frequency of the switch plate bounce mode $f_b$ and the plate thickness and modulus,

$$f_b = \sqrt{E}\,b_1\left(T + b_0\right), \tag{5}$$

where the coefficients $b_0 = 0.43613$ and $b_1 = 311.79$ are valid over the same range as $a_1$ and $a_2$. The effective mass can be found using the familiar relationship $2\pi f = \sqrt{K/M}$, so long as the static stiffness $K$ is approximately

equal to the dynamic stiffness of the system oscillating in its bounce mode only. This assumption was verified by using a Ritz, or mode-based model reduction, to find the effective stiffness and mass from the natural frequency and mode shape of the bounce mode returned by the dynamic finite element model. The stiffness and mass values thus obtained were compared with those estimated using the static stiffness and the natural frequency and found to agree to within a few percent. The equation for the effective mass is

$$M = \frac{K}{(2\pi f_b)^2} = \frac{a_2\, T\,(T - a_1)}{(2\pi b_1\,(T + b_0))^2} \tag{6}$$

where the rightmost expression is found by substituting from Eqs. (4) and (5). Histograms of $M$ and $K$, generated from 1000 samples of the independent random variables $D$, $G$, $T$ and $E$, are shown in Fig. 4 (a) and (b) respectively. Note that, by Eq. (6) and (4), $M$ and $K$ are dependent random variables. Samples of $D$, $G$, $K$ and $M$ are used to perform Monte Carlo simulations of Eqs. (1) and (2).

A value for the coefficient of restitution is also required to simulate the RF switch. This coefficient was difficult to obtain because expensive dynamic tests, using the methods in [3], are required to estimate its value, whereas the other parameters were determined using static and dimensional tests. Sensitivity studies were performed to asess the influence of the coefficient of restitution on the optimization procdure described in the next section. The optimum close waveform was not found to be particularly sensitive to the coefficient of restitution, yet the coefficient of restitution did scale the close time. This scaling effect was essentially independent of the shape of the actuation waveform. Limited experimental data and the 3D Finite Element model, both of which were described in [5,3,13] were used to estimate a realistic value for the coeff-

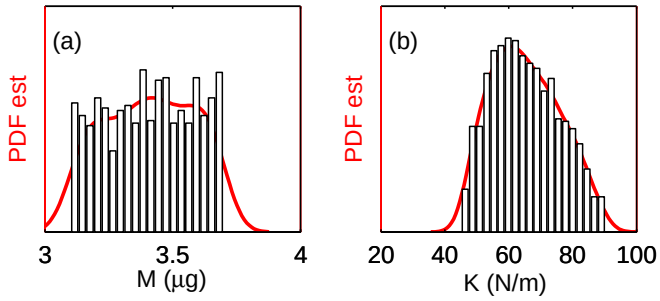


Fig. 4. *One thousand sample histograms and PDF estimates of correlated variables (a) effective mass and (b) effective stiffness, generated from the distributions shown in Figure 3.*

cient of restitution by comparing measured responses with those predicted by the 1D and 3D models and observing the effect of the coefficient on the height with which the switches rebound. The limited data suggested that a value of $\eta = 0.5$ was reasonable, so this was used in the studies that follow. This coefficient could have also been considered a random variable and included in the uncertainty model, yet this was not done because the optimum waveform did not appear to be sensitive to its value and because accurate experimental measurements on which to base an uncertainty model were not available.

## 3 Optimization

### *3.1 Performance Metrics*

The objective of waveform optimization is to minimize the impact velocity of an ensemble of RF switches with random parameters while maintaining acceptable time to closure. The maximum contact velocity $V$ for a given switch is defined as the maximum velocity $\dot{X}(t)$ at the instants $t = t_k^-, k = 1, 2, ...$ just before the switch rebounds from the contacts,

$$V = \max_{k \geq 1} \left| \dot{X}\left(t_k^-\right) \right|. \tag{7}$$

The contact velocity for the ensemble was minimized by minimizing the velocity $v_u$ of the switch at the 10% upper quantile of $V$ defined as

$$P(V > v_u) = 0.1. \tag{8}$$

The velocity $v_u$ represents the impact velocity exceeded by only 10% of the the ensemble and will be referred to as the upper velocity throughout this work. The upper velocity is estimated as

$$v_u = \hat{F}^{-1}(0.9), \tag{9}$$

where $\hat{F}$ is an approximation for the cumulative distribution function of $V$ [17].

An optimum waveform must also ensure that the probability $p_{nc}$ of a switch remaining unclosed after the voltage is applied is small. This probability was approximated as the ratio of the number of switches that did not close within 250$\mu$s to the total number of switches used in the MCS. The following objective

function accounts for both impact velocity and acceptable closure time and was used in the following section to optimize the voltage waveform

$$g = v_u + c_1 p_{nc}. \tag{10}$$

The relative importance of contact velocity and failure to close is specified by the constant $c_1 > 0$. This constant was adjusted until the desired balance between the number of unclosed switches and the time required to close the switches was achieved. A value of $c_1 = 0.0025$ cm/s gave a reasonable balance between these objectives, and will be used in all of the subsequent results. One might wish to modify this, depending on the details of screening, packaging, etc... for the application of interest.

### *3.2 Optimization Procedure*

A computational routine was created to solve the equation of motion, Eq. (1), subject to the constraint in Eq. (2) using an adaptive Runge-Kutta time integration routine. The equation of motion was solved for 200 independent realizations of the random variables $D$, $G$, $K$ and $M$ sampled from the distributions described previously. The upper velocity $v_u$ and the probability of a switch not closing $p_{nc}$ were estimated for each Monte Carlo simulation, yielding a single value for the objective function $g$ for each MCS via Eq. (10). The Monte Carlo simulation was repeated for various voltage waveforms in order to find the voltage waveform that minimized Eq. (10).

Once an upper velocity has been estimated, one can ascertain with 95% confidence that the actual probability $P_{true}(V > v_u)$ of exceeding the estimated upper velocity $v_u$ is bounded by $P_{est} - a < P_{true} < P_{est} + a$ [17]. The width of

the probability range is defined by $a$, where

$$a = 1.96\sqrt{\frac{P_{est}(1-P_{est})}{N}}, \tag{11}$$

and $N$ is the number of samples in the Monte Carlo Simulation. $N = 200$ was used in all of these simulations to give $a < 0.05$ when the estimated probability $P_{est}$ is near its nominal value of 0.1.

The voltage waveform consists of a collection of pulses where each pulse was defined by four parameters in order to reduce the dimension of the optimization problem. These parameters are illustrated in Fig. 5 for a two-pulse waveform. Each pulse $u^{(i)}$ is parameterized by its start time $t_s^{(i)}$, rise time $t_r^{(i)}$, peak time $t_p^{(i)}$ and peak voltage $u_i$ as follows

$$u\left(t\right) = \sum_{i=1}^{N} u_i \, u^{(i)}\left(t\right) \tag{12}$$

$$u^{(i)}\left(t\right) \begin{cases} \frac{1}{2} - \frac{1}{2}\cos\left(\pi \frac{t - t_s^{(i)}}{t_r^{(i)}}\right) & t_s^{(i)} \le t < t_s^{(i)} + t_r^{(i)} \\ 1 & t_s^{(i)} + t_r^{(i)} \le t < t_s^{(i)} + t_r^{(i)} + t_p^{(i)} \\ \frac{1}{2} - \frac{1}{2}\cos\left(\pi \frac{t - t_s^{(i)} - t_p^{(i)}}{t_r^{(i)}}\right) & t_s^{(i)} + t_r^{(i)} + t_p^{(i)} \le t < t_s^{(i)} + 2t_r^{(i)} + t_p^{(i)} \\ 0 & otherwise \end{cases} \tag{13}$$

The fall time of each pulse is identical to its rise time. The rise and fall of each pulse are shaped in order to limit excitation of higher frequency modes. The start time of the first pulse $t_s^{(1)}$ is set to zero. Eqs. (12) and (13) are a

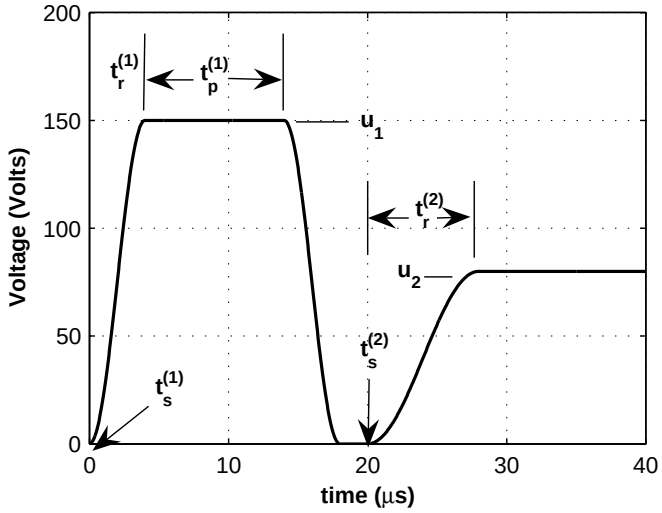


Fig. 5. *Sample actuation voltage waveform and parameter definitions.*

generalization of the pulse/coast waveform used in [5].

Initially, we restrict the analysis to waveforms with two pulses. The optimization procedure was simplified by first considering each pulse independently. The purpose of the first pulse is to bring the ensemble of switches near to the closed position with minimal velocity. Because of the nonlinear dependence of the force applied to the oscillator on $(G - X(t))^{-2}$, one would expect that longer duration forces will tend to increase the width of the distribution of the ensemble displacement and velocity. For this reason, the voltage of the first pulse was set at $u_1 = 150$ V, which is near the maximum allowable voltage, so its width could be minimum while imparting the necessary amount of energy to the switch. The rise time for this pulse was set at $t_r^{(1)} = 4\,\mu$s, which was found previously to be the fastest rise time that could be used without exciting higher modes of the switch. Its width was found by applying only the first pulse to the ensemble and increasing its width from zero (with the other parameters fixed) until about 5% of the switches impacted the contacts.

Once the peak time of the first pulse had been determined, Monte Carlo

analysis was performed for various values of $t_s^{(2)}$, $t_r^{(2)}$ and $u_2$, typically four values of $t_s^{(2)}$ and three values each of the other two, in order to obtain starting values for optimization. The set of parameters among this small group that minimized the cost function were then used as starting values for a Nelder-Mead simplex algorithm (Matlab's 'fminsearch') [18]. This algorithm varied the values for $t_p^{(1)}$, $t_s^{(2)}$, $t_r^{(2)}$ and $u_2$ until the objective function defined by Eq. (10) was minimized. This typically entailed 100-200 runs of the Monte Carlo simulation and improved the mean and upper contact velocities by about $1-2$ cm/s compared to the starting values.

The DIRECT algorithm in [19] was also applied to this problem in an effort to perform the optimization in a single step. The DIRECT algorithm is a global optimization algorithm that samples a cost function over the range of feasible input parameters, concentrating samples in the regions of the parameters space that give the best results until an optimum is obtained. Unfortunately, when applied to this problem it failed to obtain an optimum input waveform after 350 evaluations of the Monte Carlo simulation, so it was not used in the studies discussed in the next section. Instead, the simple method comprised of exhaustive search to find starting values followed by Nelder-Mead optimization that was just described was used. However, the DIRECT algorithm was helpful in finding optimum parameters for a three pulse waveform, albeit at significant computational cost, because there were too many unknown parameters to use the simple procedure described previously to obtain good starting values. Unfortunately, the three pulse waveform did not significantly reduce the contact velocity relative to the two-pulse waveform, and it was significantly more difficult to optimize its parameters, so it was abandoned.

# 4 Results

The following subsections demonstrate the performance of the ensemble of RF switches to a number of different waveforms. In Section 4.1, we design the input waveform using a deterministic model for the switch. As expected, poor performance is achieved; this scenario is presented only to illustrate what happens when we ignore the unit-to-unit variability among the MEMS devices. The input waveform is optimized in Section 4.2 assuming the unit-to-unit variability observed among the collection of RF MEMS devices is represented by the calibrated probabilistic models described in Section 2.2. Significant improvements over the results in Section 4.1 are obtained. An alternative design for the switch geometry is considered in Section 4.3, and the shape of the input waveform is optimized for this modified switch design assuming identical descriptions for the unit-to-unit variability. Lastly, in Section 4.4, we quantify the potential cost benefit of improving the repeatability of the fabrication process (decreasing the unit-to-unit variability).

## *4.1 Current Design: Input Optimized using Deterministic Model*

Before presenting the results of the waveform optimization under uncertainty, it is informative to examine the response of the ensemble of switches to a waveform that was designed using a deterministic model for the switch. A deterministic model for the switch was created by replacing the random variables, $D$, $G$, $K$ and $M$, with their mean values $E[D] = 2.43\,\mu$m, $E[G] = 3.68\,\mu$m, $E[K] = 65.3$N/m and $E[M] = 3.41\,\mu$g. A waveform was then designed to give zero contact velocity for this deterministic model using the method in [13].

The waveform is a single pulse that brings the deterministic switch to zero displacement with zero velocity, followed by a second pulse of lower amplitude that holds the switch in a closed position. This waveform was then applied to the ensemble of switches and the results are shown in Figures 6 and 7.

Figure 6 displays the voltage waveform $u(t)$ and the displacement $X(t)$ and velocity $\dot{X}(t)$ response of the ensemble of switches (defined by the distributions shown in Fig. 3) when this deterministically designed waveform is applied. For clarity, the displacement of each switch in the ensemble is shifted in Fig. 6 such that zero displacement corresponds to the closed position, so the switches start with shifted displacements equal to their random travel distance $D$ (between 2.3 and 2.7 $\mu$m). The contact velocities are clearly highest for the switches that impact the substrate first; these tend to rebound from the contacts, finally closing at about 50 $\mu$s with maximum contact velocities as high as 50cm/s. A smaller percentage of the switches do not close due the initial pulse, yet are finally attracted by the hold pulse after about one cycle (recall that the natural frequencies of the switches are about 20 kHz), closing after $60-100\,\mu$s with moderate contact velocities.

Figure 7 shows a histogram of the maximum contact velocity $V$ for the ensemble, defined in Eq. (7). A small fraction of the switches close with maximum contact velocity less than the target of 10cm/s; most have much higher contact velocities. Ninety percent of the switches close with a contact velocity less than $v_u = 42.6$cm/s while the mean contact velocity for the ensemble is 24.7cm/s.

By way of comparison, previous analysis with an unshaped waveform (where the actuating voltage jumps from 0 to 100 V at $t = 0$ and remains at that

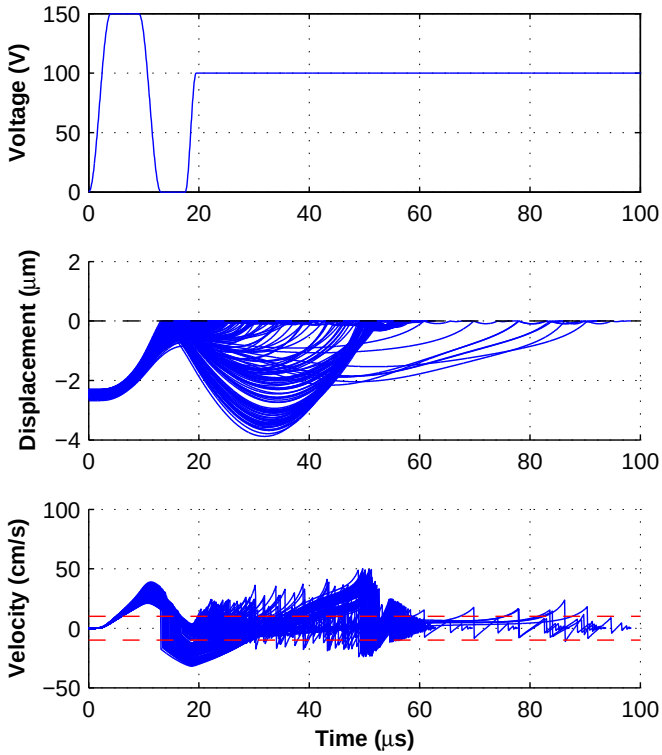


Fig. 6. *Current Design with Deterministic Model: Voltage waveform optimized for deterministic switch model and the ensemble displacement and velocity response.*

voltage thereafter) resulted in upper and mean contact velocities of $v_u = 40.7$ and 34.1cm/s respectively. The waveform in Figures 6 and 7 that is optimum in a deterministic sense actually gives a higher upper velocity than an unshaped waveform when applied to the ensemble of switches with random parameters. The contact velocities obtained using either of these waveforms are clearly unacceptable.

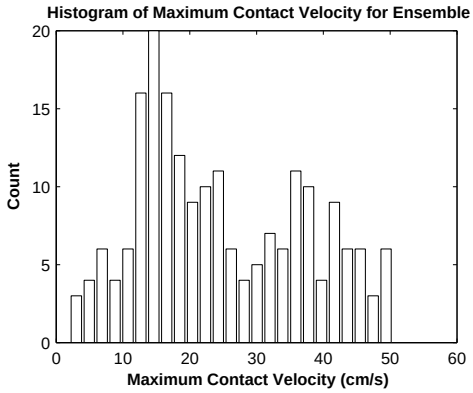


Fig. 7. *Current Design with Deterministic Model: Histogram of maximum contact velocity for the ensemble of switches using waveform optimized for deterministic switch model.*

### *4.2 Current Design: Input OUU*

The procedure described in Section 3 was applied to optimize the voltage waveform under uncertainty (OUU) using the probabilistic model for the switch that was described previously. Figure 8 displays the optimum voltage waveform $u(t)$ and the resulting ensemble response. In contrast to the results shown in Figures 6 and 7, we no longer ignore the effects of unit-to-unit variability when optimizing the waveform under uncertainty. The second pulse for the OUU waveform begins much earlier and rises much more slowly than that for the deterministically designed waveform. One would expect these features tend to increase the contact velocity for the average switch (deterministic design), yet the following figures reveal that they greatly reduce the contact velocity of the ensemble. As was the case for the deterministically designed waveform in Figure 6, a small percentage of the switches are not drawn in by the hold pulse, and finally close after $70\,\mu$s or more. However, the majority of the switches close within $50\,\mu$s with contact velocities below 25cm/s. A number of switches in Figure 6 were observed to rebound and escape the pull of the electrostatic force for a cycle, yet this is not the case for the optimum waveform in Figure 8.

Figure 9 shows a histogram of the maximum contact velocity $V$ in Eq. (7) for the ensemble of 200 switches when the optimum voltage waveform in Fig. 8 is used. Ninety percent of the switches close with a contact velocity less than $v_u = 19.7$cm/s while the mean contact velocity for the ensemble was 15.3cm/s. This represents a substantial improvement over both the waveform designed using a deterministic approach and the unshaped waveform. It is interesting to note that this waveform is not optimum in a deterministic sense since it does not result in minimum contact velocity for the switch with average parameters,

yet the maximum contact velocities experienced by the ensemble have reduced significantly.

As discussed in Section 3, a three pulse waveform was also found using the DIRECT algorithm. It gave upper and mean contact velocities of 18.8 and 14.0cm/s, so the improvement obtained by adding a third pulse did not merit the additional complexity that it introduced.

*Discussion*

One can verify that the improvement in performance observed here is statistically significant. For example, one can compute a confidence bound on the probability of obtaining a contact velocity that is higher than a certain limit using the method in [17]. Applying this to the results of the MCS, one can ascertain with 95% confidence that the probability of obtaining a contact velocity higher than 19.7cm/s using the optimum waveform is between 0.08 and 0.17, while it is between 0.50 and 0.63 for the deterministically designed waveform. Using this type of analysis, one can obtain a level of confidence in the manner with which the MCS method has solved the uncertainty problem. Then, only the system model and model reduction techniques need be questioned.

One would expect that it might be possible to reduce the contact velocity by modifying the switch design or by improving the manufacturing process to reduce the variance of the switch's parameters. Either approach changes the distributions for the system parameters. A deterministic design change entails changing the nominal value of the distributions of the parameters defining the switch. In doing so, we assume that changing the design alters only the

mean value of a given parameter, leaving the shape of the distribution and the coefficient of variation of the parameter unchanged. On the other hand, one may seek to reduce the coefficient of variation of a parameter by improving the manufacturing process. This may be more costly or difficult than a design change, but it may be necessary to meet demanding performance objectives.

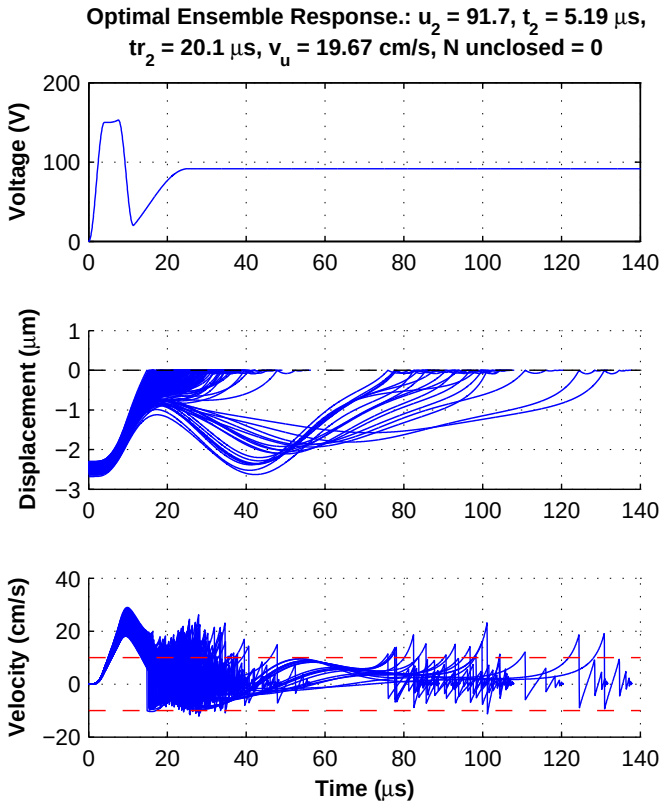


Fig. 8. *Current Design with Probabilistic Model: Voltage waveform optimized under uncertainty and ensemble displacement and velocity response.*

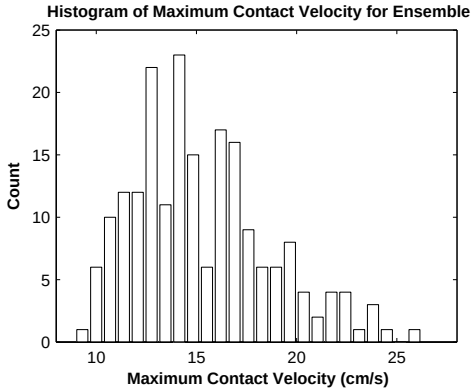


Fig. 9. *Current Design with Probabilistic Model: Histogram of maximum contact velocity for the ensemble of switches after waveform OUU.*

### *4.3 Modified Design: Input OUU*

Once the optimum waveform had been identified for the current design, the optimization methodology was then applied to study the effect of design changes on switch contact velocity. Deterministic analysis of Eq. (1) with a quasi-constant voltage $u(t)$ reveals that the system has an unstable equilibrium at $X = G/3$. The maximum value for $X$ is $D$, so the ratio $X/G$ can be no larger than $D/G$. With the current design and the bounded PDFs described previously, the switches close with $0.59 \leq D/G \leq 0.75$, which is well beyond the instability at $X/G = 1/3$. The design was modified to reduce this ratio somewhat (resulting in $0.41 \leq D/G \leq 0.52$ for the new design) and a new optimum waveform was found for the modified design. The modified design is described by a new collection of random variables $D'$, $G'$, $K'$ and $M'$, whose mean values have been altered. The new random variables are obtained from the old such that the coefficient of variation (COV) of each remains unchanged, *i.e.*,

$$Y' = \left(1 + \frac{\Delta\mu}{\mu}\right) Y, \tag{14}$$

where $Y'$ is the distribution whose mean value $\mu$ has shifted by $\Delta\mu$. By requiring the COV to remain unchanged, we do not assume that the new design can be fabricated with less variability than the current design. The $D/G$ ratio was reduced by increasing and decreasing the values of $D$ and $G$ by $0.5\,\mu$m. Such small changes were chosen so that the modified design would not deviate from the original design too drastically. The mean value of the distribution that defines the thickness of the switches was increased by $0.6\,\mu$m so the force that the leaf springs supply in the closed position would remain approximately constant. Samples of $D'$, $G'$, $T'$ and $E'$ were used to generate correlated samples for $K'$ and $M'$.

Figure 10 shows the optimum waveform and the response of an ensemble of switches with this modified design. The waveform requires a larger voltage to hold the switch closed than that in Fig. 8 since $D/G$ is smaller. Once again, the optimum waveform has a slower ramp up to the hold voltage than one would choose based on deterministic considerations. Compared to the previous cases, the percentage of switches that do not close due to the initial close pulse is smaller, yet these switches can take more than 140$\mu$s to close. The majority of the switches close within 70$\mu$s with contact velocities below 15 cm/s. The switches with the highest contact velocities seem to be those which impact the contacts before 20 $\mu$s, rebound, and impact again with higher velocity between $25 - 30\,\mu$s.

Figure 11 shows a histogram of the maximum contact velocity. The upper and mean contact velocity have reduced to $v_u = 12.5$cm/s and 10.7cm/s respectively, a reduction of more than 30% compared to the OUU waveform for the current design in Section 4.2, or about a 50% improvement relative to either the unshaped or deterministically designed waveforms.

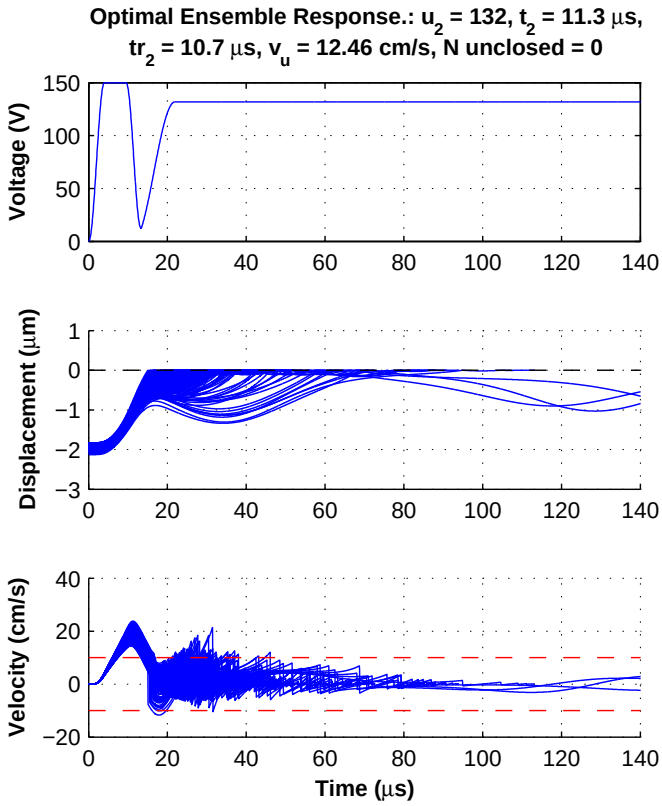


Fig. 10. *Modified Design with Probabilistic Model: Voltage waveform optimized under uncertainty and resulting ensemble displacement and velocity response.*

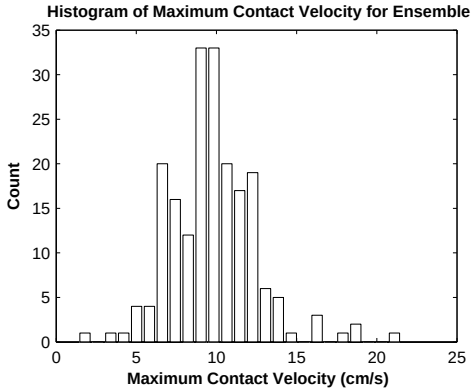


Fig. 11. *Modified Design with Probabilistic Model: Histogram of maximum contact velocity for the ensemble of switches after waveform OUU.*

### *4.4 Current Design with Process Repeatability Improved: Input OUU*

The effect of manufacturing process repeatability on impact velocity was also investigated. This information was sought to assess the cost-versus-benefit realized by improving process repeatability. This was studied by changing the coefficient of variation (COV) of each random variable and then finding a new optimum waveform for the improved process. Let $Y$ be a random variable with mean $\mu \neq 0$, standard deviation $\sigma > 0$ and COV $\sigma/\mu$. The COV can be modified by $0 < \Delta\sigma < 1$ using the following change of variables

$$Y'' = \mu(1 - \Delta\sigma) + \Delta\sigma Y. \tag{15}$$

New distributions for the switch model parameters $D''$, $G''$, $K''$ and $M''$ were generated by assuming a 50% reduction in the COV of the switch thickness, gap distance and travel distance ($\Delta\sigma = 0.5$) from the current design. A histogram of the maximum contact velocities after optimizing the waveform for the modified parameter distributions is shown in Fig. 12. This ensemble of switches achieves upper and mean maximum contact velocities of 12.8cm/s and 9.6cm/s respectively, an improvement of 35% over the current design in Section 4.2. This type of analysis provides management with a quantified measure of the expected gains in design performance due to an investment that improves process repeatability.

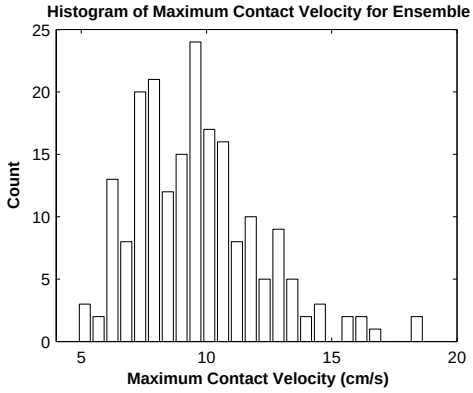


Fig. 12. *Current Design with Process Repeatability Improved: Histogram of maximum contact velocity for the ensemble of switches for current design after waveform OUU.*

## 5 Conclusions

This work has demonstrated input waveform optimization under uncertainty for a highly nonlinear, electro-statically actuated radio-frequency MEMS switch. A reduced order model for the switch, including an uncertainty model based on experimental data and expert opinion, was used in a Monte Carlo simulation that predicted the maximum impact velocity experienced by an ensemble of switches subjected to an input waveform. The shape of the waveform was then optimized to minimize the contact velocity for the ensemble of switches, resulting in a 50% reduction in the overall contact velocity when compared to an unshaped waveform. Care was taken to assure that the majority of switches closed in a reasonable amount of time by adjusting the weighting given to the number of switches that close within a certain time and the contact velocity. The optimization procedure was used to predict the reduction in contact velocity that could be obtained by modifying the design of the switch. One design and its corresponding optimum waveform were presented that reduced the contact velocity by 30% relative to the optimum waveform for the current design. These results are summarized in Fig. 13. The improvement obtained by optimizing the waveform while considering uncertainty is substantial. It is also interesting to note that none of the estimated PDFs appears to have a standardized form. Considerable errors might have been obtained if a statistical method were used that assumes a form for the distribution of the output.

Other modifications of this class are currently being investigated considering all of the manufacturing and electrical performance constraints on the switches. The optimization procedure was also used to predict the effect of improving the repeatability of the manufacturing process on the contact ve-

locity, revealing that a 50% improvement in repeatability resulted in a 35% reduction in the contact velocity of the ensemble of switches. This information is valuable when performing cost-benefit analyses to justify future investments to improve the fabrication process and to allocate project resources between design and process improvement.

All of these analyses would have been computationally intractable if a low order, computationally efficient model for the switches had not been available. An adequately accurate model for the switches was derived using classical model reduction techniques and physical insight. The expected accuracy of this model can be established to a significant degree by considering the effect of the nonlinear contact forces and the input voltage waveform on the otherwise linear switches, as was discussed, so the limitations of the model are relatively well understood. (This model was also validated previously using experimental measurements on actual switches [13,5,3].)

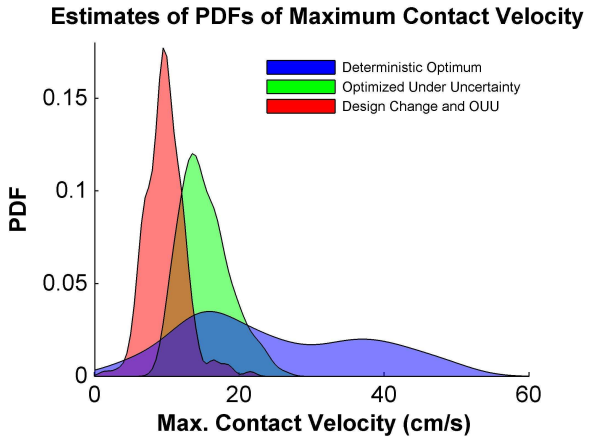


Fig. 13. *Estimates of the probability density functions of contact velocity for the ensemble of switches using 1.) waveform optimized for deterministic model, 2.) the waveform optimized under uncertainty for current design, and 3.) waveform optimized under uncertainty after modifying the switch design.*

The effort that was applied to derive and validate a simple, low-order model paid large dividends since the Monte Carlo Simulation (MCS) technique could be applied to perform uncertainty analysis. MCS requires no *a priori* assumptions about the character of the uncertainty problem, so the results obtained are true to the model and their expected variance could be computed. Conversely, many of the methods discussed in the introduction, such as FORM and SORM, make assumptions regarding the mathematical form of the uncertainty problem that cannot be evaluated unless a trusted sampling method such as MCS is also applied. One should also note that the detailed information that was obtained regarding the diverse phenomena experienced by the ensemble of switches would typically not have been obtained if a reliability method had been employed, once again highlighting the utility of Monte Carlo Simulation in this application.

## 6 Acknowlegements

The authors gratefully acknowledge the technical contributions of William D. Cowan in this work.

## References


[1] G. M. Rebeiz, RF MEMS Theory, Design and Technology, Wiley, 2003.

[2] J. Yao, RF MEMS from a device perspective, J. Micromech. Microeng. 10 (2000) R9–R38.

[3] H. Sumali, J. E. Massad, D. A. Czaplewski, C. W. Dyck, Waveform design for pulse-and-hold electrostatic actuation in MEMS, Sensors and Actuators A (Physical) 134 (1) (2007) 213–20.

[4] K. Maute, D. M. Frangopol, Reliability-based design of MEMS mechanisms by topology optimization, Computers and Structures 81 (2003) 813–824.

[5] D. Czaplewski, C. Dyck, H. Sumali, J. Massad, J. Kuppers, I. Reines, W. Cowan, C. Tigges, A soft landing waveform for actuation of a single pole single throw Ohmic RF MEMS switch, Journal of Micromech. Sys., 2006, vol.15, no.6, p.1586-94.

[6] H. O. Madsen, First order vs. second order reliability analysis of series structures, Structural Safety 2 (3) (1985) 207–214.

[7] J. S. Han, B. M. Kwak, Robust optimization using a gradient index: MEMS applications, Struct Multidisc Optim 27 (2004) 469–478.

[8] J. W. Wittwer, M. S. Baker, L. L. Howell, Robust design and model validation of nonlinear compliant micromechanisms, Journal of Microelectromechanical Systems 15 (1) (2006) 33–41.

[9] M. Allen, M. Raullin, K. Maute, D. M. Frangopol, Reliability-based analysis and design optimization of electrostatically actuated MEMS, Computers and Structures 82 (2004) 1007–1020.

[10] W. Singhose, L. Pao, Comparison of input shaping and time-optimal flexible-body control, Control Engineering Practice 5 (4) (1997) 459–467.

[11] P. H. Meckl, W. P. Seering, Controlling velocity-limited systems to reduce residual vibration., in: Proceedings - 1988 IEEE International Conference on Robotics and Automation., IEEE, New York, NY, USA, Philadelphia, PA, USA, 1988, pp. 1428–1433 BN – 0–8186–0852–8.

[12] C. Dyck, T. A. Plut, C. D. Nordquist, P. S. Finnegan, F. Austin, I. Reines, Fabrication and characterization of Ohmic contacting RF MEMS switches, in: SPIE Conference on Micromachining and Microfabrication, Vol. 5344, 2004, pp. 79–88.

[13] J. Massad, H. Sumali, D. S. Epp, C. Dyck, Modeling, simulation, and testing of the mechanical dynamics of an RF MEMS switch, in: Proceedings of the 2005 International Conference on MEMS, NANO and Smart Systems (ICMENS05), 2005, pp. 237–240.

[14] J. H. Ginsberg, Mechanical and Structural Vibrations, 1st Edition, John Wiley and Sons, New York, 2001.

[15] H. Sumali, J. Kuppers, D. Czaplewski, J. Massad, C. Dyck, Structural dynamics of an RF MEMS switch, in: 2005 ASME International Mechanical Engineering Congress and Exposition (IMECE), Orlando, Florida, USA, 2005.

[16] R. V. Field, D. S. Epp, Development and calibration of a stochastic dynamics model for the design of a MEMS inertial switch, Sensors and Actuators A: Physical 134 (1) (2007) 109–118.

[17] A. Ang, W. Tang, Probability Concepts in Engineering Planning and Design: Vol. 1 - Basic Principles, John Wiley and Sons, Inc., New York, NY, 1975.

[18] J. C. Lagarias, J. A. Reeds, M. H. Wright, P. E. Wright, Convergence properties of the Nelder-Mead simplex method in low dimensions, SIAM J. OPTIM. 9 (1) (1998) 112–147.

[19] C. Perttunen, D. Jones, B. Stuckman., Lipschitzian optimization without the Lipschitz constant, Journal of Optimization Theory and Application 79 (1) (1993) 157–181.